High−Affinity and Cooperative Binding of Oxidized Calmodulin by Methionine Sulfoxide Reductase †

ARTICLE *in* BIOCHEMISTRY · JANUARY 2007

Impact Factor: 3.02 · DOI: 10.1021/bi0612465 · Source: PubMed

8 AUTHORS, INCLUDING:

Heather S Smallwood
The University of Tennessee Health Science …
20 PUBLICATIONS **446** CITATIONS
SEE PROFILE

Ramona J Bieber Urbauer
University of Georgia
39 PUBLICATIONS **962** CITATIONS
SEE PROFILE

Nadezhda Galeva
University of Kansas
49 PUBLICATIONS **909** CITATIONS
SEE PROFILE

Todd D Williams
University of Kansas
133 PUBLICATIONS **4,112** CITATIONS
SEE PROFILE

High-Affinity and Cooperative Binding of Oxidized Calmodulin by Methionine Sulfoxide Reductase†

Yijia Xiong,‡ Baowei Chen,‡ Heather S. Smallwood,‡ Ramona J. Bieber Urbauer,# Lye Meng Markille,‡ Nadezhda Galeva,§ Todd D. Williams,§ and Thomas C. Squier*,‡

Biological Sciences Division, Pacific Northwest National Laboratory, Richland, Washington 99354, Department of Biochemistry and Molecular Biology, University of Georgia, Athens, Georgia 30602, and Mass Spectrometry Laboratory, University of Kansas, Lawrence, Kansas 66045

Received June 22, 2006; Revised Manuscript Received September 21, 2006

ABSTRACT: Methionines can play an important role in modulating protein−protein interactions associated with intracellular signaling, and their reversible oxidation to form methionine sulfoxides [Met(O)] in calmodulin (CaM) and other signaling proteins has been suggested to couple cellular redox changes to protein functional changes through the action of methionine sulfoxide reductases (Msr). Prior measurements indicate the full recovery of target protein activation upon the stereospecific reduction of oxidized CaM by MsrA, where the formation of the S-stereoisomer of Met(O) selectively inhibits the CaM-dependent activation of the Ca-ATPase. However, the physiological substrates of MsrA remain unclear, as neither the binding specificities nor affinities of protein targets have been measured. To assess the specificity of binding and its possible importance in the maintenance of CaM function, we have measured the kinetics of repair and the binding affinity between oxidized CaM and MsrA. Reduction of Met(O) in fully oxidized CaM by MsrA is sensitive to the protein fold, as repair of the intact protein is incomplete, with >6 Met(O) remaining in each CaM following MsrA reduction. In contrast, following proteolytic digestion, MsrA is able to fully reduce one-half of the oxidized methionines, indicating that surface-accessible Met(O) within folded proteins need not be substrates for MsrA repair. Mutation of the active site (i.e., C72S) in MsrA permitted equilibrium-binding measurements using both ensemble and single-molecule fluorescence correlation spectroscopy measurements. We observe cooperative binding of two MsrA to each CaM_{ox} with an apparent affinity ($K = 70 \pm 10$ nM) that is 3 orders of magnitude greater than the Michaelis constant ($K_M = 68 \pm 4$ μM). The high-affinity and cooperative interaction between MsrA and CaM_{ox} suggests an important regulatory role of MsrA in the binding and reduction of Met(O) in functionally sensitive proteins, such that multiple MsrA proteins are recruited to simultaneously bind and reduce Met(O) in highly oxidized proteins. Given the suggested role of Met(O) in modulating reversible binding interactions between proteins associated with cellular signaling, these results indicate an ability of MsrA to selectively reduce Met(O) within highly surface-accessible sequences to maintain cellular function as part of an adaptive response to oxidative stress.

In response to environmental stressors, methionine residues in proteins can be oxidized to methionine sulfoxides [Met(O)] by reactive oxygen species (ROS[1]) and have the potential to modulate protein function and intracellular signaling (*1*−*6*). Indeed, under basal conditions between 4 and 9% of all methionines (depending on tissue source) are oxidized to their corresponding methionine sulfoxides (*7*), emphasizing the sensitivity of methionine residues to oxidation. Oxidation-dependent changes in protein function are reversible, as endogenous Met(O) reductases (Msr) can catalyze the reduction of free and protein-bound Met(O) (*8*). This repair process is dependent on cellular redox conditions through the action of thioredoxin reductase, which uses NADPH to reduce surface-exposed cystine residues in Msr through thioredoxin and thioredoxin reductase (*9*, *10*).

The important role played by methionines in mediating reversible binding interactions between proteins was first suggested by Bernstein and co-workers, who noted an important role for methionine-rich sequences in mediating intermolecular recognition and binding to a wide variety of different nonpolar peptide sequences (*11*). Subsequently, DeGrado and co-workers clarified the structural role of methionine-rich binding pockets in calmodulin (CaM), which are thought to permit the selective association with divergent

† This work was supported by grants from the National Institutes of Health (NIA AG12993 and AG17996).

* To whom correspondence should be addressed. Thomas C. Squier, Cell Biology and Biochemistry Group, 790 6th St., Mail Stop P7-53, Pacific Northwest National Laboratory; Richland, Washington 99354. Tel: (509) 376-2218; fax: (509) 376-6767; e-mail: thomas.squier@pnl.gov.

‡ Pacific Northwest National Laboratory.

University of Georgia.

§ University of Kansas.

[1] Abbreviations: CaM, calmodulin; CaM_{ox}, oxidized calmodulin; Alexa532, Alexa Fluor 532; DTT, dithiothreitol; EGTA, ethylene glycol-bis(β-aminoethyl ether)-*N*,*N*,*N*′*N*′-tetraacetic acid; FCS, fluorescence correlation spectroscopy; HEPES, [4-(2-hydroxyethyl)piperazino]ethanesulfonic acid; MOPS, 3-(*N*-morpholino)propane-sulfonic acid; Tris, (hydroxymethyl)aminomethane; Msr, methionine sulfoxide reductase; MsrC72S, mutant of Msr where the active site cysteine was mutated into a serine; ROS, reactive oxygen species.

10.1021/bi0612465 CCC: $33.50
Published on Web 11/17/2006

CaM-binding sequences as a result of both their larger polarity and conformational flexibility relative to other hydrophobic residues (*12*, *13*). Additional understanding of the structural underpinning for this observation was described by Gellman (*14*), who emphasized two additional properties of Met that promote the sequence-independent recognition between nonpolar protein surfaces, which promotes the structural plasticity associated with molecular recognition common in intracellular signaling. First, the presence of the sulfur atom facilitates the flexibility of the methionine side chain by reducing the enthalpic discrimination among the possible χ_3 torsion angles, "permitting surfaces containing this residue to have considerable freedom to mold themselves to accommodate nonpolar binding partners of varying structures" (*14*). Second, the greater polarizability of the thioether sulfur atom in Met in comparison to typical hydrocarbons enhances binding to nonpolar surfaces. Further, reversible binding interactions between proteins can be selectively modulated through the reversible oxidation of surface-exposed methionines to their corresponding methionine sulfoxides, which will affect the energetics of the binding interface (*14*). This latter suggestion has been extensively validated in the case of CaM, where Met oxidation can disrupt a majority of the binding interactions with target proteins (*15*). Thus, the accumulation of oxidized methionines in CaM and other proteins during biological aging may be sensitive to diminished cellular redox conditions and can contribute to a loss of cell function (*16*, *17*). Indeed, CaM isolated from the long-lived hybrid strains of rodents is not oxidized in aged animals (*18*), suggesting that the ability to maintain reduced CaM may contribute to healthy aging. Consistent with this latter suggestion, Msr activities are essential for optimal cell function, and strong correlations are observed between genetic manipulations that modify Msr function and the resistance to oxidative stress and lifespan (*19*, *20*). Indeed, age-dependent declines in MsrA activity correlate with multiple age-related diseases, including Alzheimer's and Parkinson's disease (*21*−*24*).

Reduction of the S- and R-stereoisomers of Met(O) involves two complementary proteins, MsrA and MsrB (*25*, *26*). While MsrA and MsrB have little sequence homology, the active sites of these enzymes are mirror images, consistent with their complementary stereochemical repair specificities (*8*, *25*, *27*−*30*). The catalytic mechanism of reduction has been most extensively studied for MsrA, whose catalytic activity is significantly greater than that of MsrB (*29*). The active site of MsrA is a highly conserved Gly-Cys^{72}-Phe-Trp-Gly motif; mutations of the active site cysteine (i.e., Cys^{72}) or either of the proximal hydrophobic side chains result in a complete loss of reduction activity (*9*, *31*). Enzyme catalysis occurs through a series of thiol-disulfide exchange steps, which are proposed to involve a "Ping-Pong" mechanism, whereby following the reduction of Met(O) the catalytic cysteine (i.e., Cys^{72}) in MsrA forms a sulfenic acid intermediate that is subsequently reduced through the formation of an intradisulfide bond involving either Cys^{218} or Cys^{227} (*9*). Subsequent binding and reduction of the disulfide is mediated by thioredoxin, which has been suggested to represent the rate-limiting step of the reaction (*27*, *29*).

To understand the functional regulation and binding specificity of MsrA from eukaryotes and its possible involvement in the reduction of oxidized CaM (CaM_{ox}) under conditions of oxidative stress, we have expressed and purified both wild-type and a mutant bovine MsrA in which the active site cysteine at position 72 was changed to serine (i.e., MsrA-C72S), permitting both functional activity assays and binding measurements of MsrA affinity. Using mass spectrometry, we have identified the structural requirements of the recognition motif surrounding oxidized methionines, which must be surface exposed and conformationally disordered. The K_M associated with the reduction of CaM_{ox} is 68 ± 4 μM, indicating the reduction of protein bound Met(O) is physiologically relevant. Using fluorescence spectroscopy, we have measured the binding affinity of MsrA-C72S to CaM_{ox} ($K = 70 \pm 10$ nM), which is substantially less than K_M and is consistent with earlier suggestions that the rate-limiting step involves the reduction of the disulfide in Msr following the release of the reduced methionine from the substrate (*29*). Binding is not dependent on the redox state of MsrA. These latter results suggest that in addition to the reduction of Met(O) an additional function of MsrA may be to minimize the aggregation of CaM_{ox} and other cellular proteins under conditions of oxidative stress.

EXPERIMENTAL PROCEDURES

Materials. SDS polyacrylamide gels were obtained from Bio-Rad (Hercules, CA). Protein ladder molecular weight markers, rhodamine 6G, and Alexa Fluro 532 (Alexa532) were from Invitrogen (Carlsbad, CA). Hydrogen peroxide (H_2O_2) was obtained from Fisher (Pittsburgh, PA), and the concentration was determined using the published extinction coefficient $\epsilon_{240} = 39.4 \pm 0.2$ M^{-1} cm^{-1} (*32*). A micro BCA protein assay reagent kit was obtained from Pierce Chemical Co. (Rockford, IL). Type XIII TPCK-treated trypsin and type I-S soybean trypsin inhibitor were obtained from Sigma (St. Louis, MO). Glutathione Sepharose 4B was obtained from Pharmacia Biotech (Sweden). All other chemicals were the purest grade commercially available. A single isoform of CaM corresponding to the cDNA encoding vertebrate CaM provided by Professor Sam George (Duke University) was subcloned into the expression vector pALTER-Ex1 (Promega, Madison, WI), overexpressed in *Escherichia coli* strain JM109 (Promega, Madison, WI), and purified essentially as previously described using phenyl Sepharose CL-4B (Pharmacia, Piscataway, NJ) and weak anion exchange HPLC (*33*, *34*). Methionines in CaM were oxidized upon incubation with 60 μM CaM (1 mg/mL) in 1.0 mM imidazole (pH 6.5), 10 mM $CaCl_2$, and 100 mM KCl with 100 mM H_2O_2 for 24 h at room temperature. The reaction was stopped by dialyzing the sample against multiple changes of distilled water buffered with sodium bicarbonate at 4 °C. Purified proteins were stored at −80 °C.

Cloning and Mutagenesis of the msrA Gene. To allow ease of purification, a poly histidine tag and linker (MGHHHHHHHHHHSSGHIEGRH) was added to the N-terminus of MsrA for protein overexpression in *E. coli*, essentially as described by Lowther and co-workers (*9*). The plasmid, pGEX-MsrA, containing the complete cDNA sequence of the gene encoding for bovine MsrA, was provided by Professor Nat Brot (*35*) and used as template for PCR. Upper (5′-GCGTGGA**CATATG**CTCTCG GTCACCAGGAG-3′) and lower (5′ GCG**CTCGAG**TTACTTTTTAATACCCAG-3′) oligonucleotide primers were synthesized by Invitrogen (Carlsbad, CA) and used to PCR amplify a 721 bp fragment

corresponding to the *msrA* gene. *Nde*I and *Xho*I restriction sites were added at the 5′ and 3′ end of the gene (bold), respectively, to facilitate cloning. The PCR fragment was cloned into pBluescript II SK (Stratagene, La Jolla, CA), which was previously modified to incorporate an *Nde*I restriction site, and transformed into *E. coli* strain XL1-Blue MRF' (Stratagene) using standard molecular biology techniques (*36*). Plasmid DNA was extracted from a representative fraction of transformants using QIAprep Spin Miniprep kit (Qiagen, Inc., Valencia, CA) and submitted for DNA sequencing (Biochemical Research Service Laboratory, University of Kansas, Lawrence, KS). The sequence of the cloned *msrA* gene was confirmed, subcloned into the *Nde*I and *Xho*I restriction sites of the expression vector, pET-16b (EMD Biosciences, San Diego, CA), and transformed into *E. coli* strain DH5a (Invitrogen) using standard methods (*36*). Transformants were screened as described previously. One clone was selected and transformed into *E. coli* strain BL21-(DE3) (EMD Biosciences) for expression of the *msrA* gene. To create the inactivated MsrA protein, residue 72 was mutated from cysteine to serine in the wildtype *msrA* gene using a method previously described (*37*, *38*). Briefly, upper (5′-AATGGGA**TCC**TTCTGGGGAGCTGAAAG-3′) and lower (5′-CCGAATACAGCCATCTGTGTTCCCTCTG-3′) oligonucleotide primers were synthesized by MWG Biotech Inc. (High Point, NC), incorporating the serine codon at position 72 in the upper primer (bold). The plasmid, pBluescript II SK, containing the wild-type *msrA* gene was used as template in the PCR reactions. The PCR reactions were transformed into *E. coli* strain DH10B (Invitrogen) and transformants were screened and submitted for DNA sequencing (Iowa State University DNA Sequencing and Synthesis Facility, Ames, IA). The sequence of the mutated *msrA* gene (*C72S-msrA*) was confirmed and subcloned into the expression vector, pET-16b, as before. One clone was selected and transformed into *E. coli* strain BL21(DE3) for expression of the *C72S-msrA* gene. Both MsrA and C72S-MsrA proteins are expressed with an N-terminal His_{10} tag.

Expression and Purification of MsrA and C72S-MsrA. For overexpression of both MsrA and C72S-MsrA proteins, 1.0 L of Luria broth (LB) supplemented with carbenicillin (100 mg/mL) (Sigma-Aldrich, St. Louis, MO) was inoculated with a 40 mL overnight culture and incubated shaking at 250 rpm and 37 °C. During incubation, the optical densities (OD) of the bacterial cultures were monitored at 600 nm. When the OD reached ~0.8, isopropyl-b-D-thiogalactopyranoside (IPTG) was added to a final concentration of 1 mM to induce expression of MsrA and C72S-MsrA. Incubation continued at 250 rpm and 37 °C. After 5 h incubation, the cells were pelleted by centrifugation at 4000*g* for 15 min at 4 °C, resuspended in lysis buffer (50 mM NaH_2PO_4, 300 mM NaCl, 10 mM imidazole, pH 8.0), lysed with 150 mg/mL lysozyme, and sonicated. The suspension was centrifuged at 15000*g* for 30 min at 4 °C. Column chromatography was performed at 4 °C. The crude lysis supernatant solution was applied to a Ni-NTA His-Bind Superflow (EMD Biosciences) column (1.5 × 20 cm) equilibrated with lysis buffer. The column was washed extensively with lysis buffer, followed by another wash with lysis buffer containing 20 mM imidazole. MsrA and C72S-MsrA were eluted with 50 mM NaH_2PO_4 (pH 8.0), 300 mM NaCl, 250 mM imidazole. Protein concentrations were determined using the absorbance, where $\epsilon_{280\ nm} = 31\ 390\ M^{-1}\ cm^{-1}$ (*9*) or using the Coomassie Plus Bradford reagent from Pierce (Rockland, IL) using albumin as a standard.

Cloning and Expression of MsrBA. A 903-bp PCR fragment encoding the gene for MsrBA from *Shewanella oneidensis* MR1 was amplified using the following primers, MSRBAF (5′-CACCATGGACAAACTGACTGATTTTG-AA3′) and MSRBAR (5′-AACTTGCAGTTCGGCAA ATA-AAT GC-3′), and cloned into a pENTR/SD/D-TOPO vector (Invitrogen, Carlsbad, CA) and transformed into *E. coli* strain Top10. Clones were screened, and positive clones were verified by DNA sequencing (Amplicon Express, Pullman, WA). To overexpress recombinant MsrBA protein, the MsrBA/pENTR construct was cloned into pETDEST 42 (Invitrogen) using LR Clonase and transformed into *E. coli* strain BL21Star(DE3). This construct encoding MsrBA produced a fusion protein containing a V5 epitope and a His_6 tag at the C-terminus, which enables purification by TALON metal affinity column chromatography (Clontech, Mountain West, CA). Following induction using isopropyl-β-D-thigalactopyranoside (IPTG), bacteria were harvested by centrifugation, and cells were lysed by three passes through a French pressure cell. Following removal of cell membranes by centrifugation, the supernatant was loaded onto a cobalt affinity column (BD Biosciences, Palo Alto, CA). Following extensive washing with a buffer containing 10 mM Tris-HCl (pH 8.0), 300 mM NaCl, and 20 mM imidazole, purified MsrBA was eluted with 25 mL of 10 mM Tris-HCl (pH 8.0), 300 mM NaCl, and 300 mM imidazole. Msr concentrations were determined by Pierce Coomassie Plus Protein assay (Pierce Chemical Co., Rockford, IL).

CaM_{ox} Repair by MsrA. To measure the repair of oxidized CaM by MsrA, 10 μM CaM_{ox} was incubated with 1.0 μM MsrA or MsrBA in 10 mM MOPS (pH 7.5), 50 mM KCl, and 15 mM DTT for 12 h at 25 °C. In some measurements, CaM_{ox} was first digested with trypsin in 50 mM Tris·Cl (pH 7.5) using a weight ratio of 1−100 and incubated at 37 °C overnight. Following the addition of 1.8 μM trypsin, rates of Met(O) reduction were measured upon addition of MsrA. Alternatively, reactions were carried out in 10 mM Tris-HCl buffer (pH 7.5) using 400 μM NADPH, 2.0 μM thioredoxin reductase, and the indicated concentrations of thioredoxin and CaM, permitting the enzymatic activity of MsrA to be measured by changes in NADPH absorption at 340 nm ($\epsilon_{340\ nm} = 6220\ M^{-1}\ cm^{-1}$) (*39*).

Fluorescent Labeling. CaM was covalently labeled using either Alexa488 or Alexa532 from Molecular Probes. Briefly, CaM (1.0 mg) in 0.5 mL of 0.1 M Na_2CO_3 (pH 8.3) was incubated with either Alexa probe for 1 h at 20 °C, and unbound dye was removed using a G-25 Sephedex column. Stoichiometries of binding were determined by measuring the absorbances at 280 nm and either 495 nm (Alexa488) or 530 nm (Alexa532), where $\epsilon_{280\ nm} = 2560\ M^{-1}\ cm^{-1}$ for CaM, $\epsilon_{488\ nm}$ (Alexa488) $= 71\ 000\ M^{-1}\ cm^{-1}$, and $\epsilon_{532\ nm}$ (Alexa532) $= 81\ 000\ M^{-1}\ cm^{-1}$ (*40*, *41*). The final molar stoichiometry was ~1 mol of bound fluorophore per mole of CaM.

Fluorescence Correlation Spectroscopy Measurements. Fluorescence correlation spectra (FCS) were obtained using a Nikon TE300 inverted microscope modified for these measurements, where excitation of Alexa532 was from a Coherent Verdi laser (532 nm) attenuated by a circular

neutral density filter and focused by a 100× objective lens (S Fluo100, Nikon, Japan) 50 μm above the surface of the cover slide. The fluorescence was collected using the same objective, separated by a 550DCLP dichroic mirror (Chroma Technology, Brattleboro, VT). A 50-μm diameter pinhole was installed in the image plane of the output fluorescence to get rid of the out-of-focus signal. To minimize the effect of after pulse, the fluorescence was split by a cube beam splitter (Thorlabs, Newton, NJ), and detected subsequent to a HQ560 emission filter using a pair of SPCM-AQR-14 avalanche photodiodes (Perkin-Elmer Optoelectronics, Vaudreuil, Canada). The output was fed into a Flex01-05D multi-tau correlator (Correlator.com, Bridgewater, NJ), and the fluorescence correlation function was calculated in real time. Alternatively, a two-photon excitation configuration was used for the excitation of Alexa488-labeled CaM involving the output from a Mira 900 Ti:Sapphire femtosecond laser (Coherent) (780 nm) using a 675dcsx4 dichroic and e700sp-2p8 short-pass blocking filter and an HQ535 emission filter. All mirrors were from Chroma Technology.

Unless otherwise stated, all FCS measurements involved either Alexa488- or Alexa532-labeled CaM (5 nM) in 20 mM HEPES buffer (pH 7.5), 100 mM KCl, 1.0 mM $MgCl_2$, and 0.2 mM EGTA in the absence and presence of 1.0 mM $CaCl_2$ at 20 °C, where the concentration of MsrA-C72S was varied between 0 and 500 nM. When indicated, 15 mM DTT were added to reduce MsrA. Prior to all measurements, the cover slides (Fisher premium cover glass) were cleaned for 30 min in a 10% (w/v) NaOH solution using a Branson 200 sonicator. A 100-μL droplet of the sample solution was placed on a clean cover slide. Typically, data were collected for 30 s, and 5−15 replicates were measured for each sample. Evaluation of the curves was carried out using the nonlinear fitter in ORIGIN (MicroCal Software, Northampton, MA).

FCS Theory. The autocorrelation function $G(\tau)$ is the sum of two species of fluorescent molecules.

$$G(\tau) = 1 + \left(1 + \frac{f_T}{1-f_T} e^{-\tau/\tau_T}\right)\frac{1}{N}\left[\frac{\alpha}{\left(1+\frac{\tau}{\tau_{D1}}\right)\times\sqrt{1+\left(\frac{\omega}{z}\right)^2\left(\frac{\tau}{\tau_{D1}}\right)}} + \frac{1-\alpha}{\left(1+\frac{\tau}{\tau_{D2}}\right)\times\sqrt{1+\left(\frac{\omega}{z}\right)^2\left(\frac{\tau}{\tau_{D2}}\right)}}\right] \quad (1)$$

N is the total number of fluorescent molecules within the focal point, f_T and τ_T are the fractional population and decay time of the triplet state, respectively; ω and z are the radial and axial radii of the confocal volume, respectively, τ is the lag time between two channels, α is the fraction of unbound CaM_{ox}, and τ_{D1} and τ_{D2} are the apparent diffusion times of unbound CaM_{ox} and the complex containing MsrA bound to CaM_{ox}. The ratio, ω/z, is a structural parameter of a FCS setup and is calibrated using rhodamine 6G, whose diffusion coefficient is 2.8×10^{-10} m^2 s^{-1} (*42*). The relation between the diffusion time (τ_{Di}) and translational diffusion coefficient (D_i) is

$$D_i = \frac{\omega^2}{4 \times \tau_{D_i}} \quad (2)$$

The Stokes−Einstein formula can be used to estimate the hydrodynamic radius (R) of the complex assuming a spherical particle, where

$$R_i = \frac{kT}{6\pi\eta D_i} \quad (3)$$

k is the Boltzmann constant (1.38×10^{-23} J/K), T is the absolute temperature, (293 K), η is the viscosity of water (0.89 cP). From the hydrodynamic radius of the molecule the molecular mass (m) can be calculated.

$$m = 4\pi\rho N_A R^3/3 \quad (4)$$

where N_A is Avogadro's number, and ρ is the mean density of the molecule.

Binding Affinity Between CaM_{ox} and MsrA. The fluorescence autocorrelation curves were fitted simultaneously using eq 1 to obtain the fraction of bound CaM_{ox} (i.e., $1 - \alpha$) at each concentration of MsrA-C72S, and the resulting binding curve was fit using the Hill equation:

$$\frac{(1-\alpha)}{(1-\alpha)_{max}} = \frac{[MsrA]^n}{K^n + [MsrA]^n} \quad (5)$$

where n is the Hill coefficient and K is the macroscopic dissociation constant, which represents the sum of the microscopic equilibrium binding constants (i.e., $k_1 + k_2$) for homotropic cooperativiity (*43*), where

$$CaM + MsrA \leftarrow k_1 \rightarrow CaM{:}MsrA + MsrA \leftarrow k_2 \rightarrow CaM{:}MsrA_2 \quad (6)$$

Further consideration of the mechanism underlying cooperative binding is possible, where

$$\frac{(1-\alpha)}{(1-\alpha)_{max}} = \frac{K_1[MsrA] + 2K_2[MsrA]^2}{2(1 + K_1[MsrA] + K_2[MsrA]^2)} \quad (7)$$

The macroscopic equilibrium association constant K_1 corresponds to the sum of the two intrinsic equilibrium constants (k_1 and k_2) associated with MsrA binding to CaM_{ox} and K_2 corresponds to the product of the equilibrium constants associated with binding to both sites and includes contributions

$$K_c = \frac{4K_2}{K_1^2}. \quad (8)$$

associated with cooperativity (i.e., $k_1k_2k_{12}$) (*44*). A lower estimate of the contribution of the cooperative interaction is possible by assuming that $k_1 = k_2$.

Mass Spectrometric Analysis. Intact CaM samples were loaded onto a C_{18} trap column with 1% aqueous acetic acid for desalting and then eluted with 90:9.5:0.5 methanol/H_2O/formic acid (v/v/v) at 20 μL/min into the source of a Q-TOF2 mass spectrometer (Micromass LTD, UK). Acquired intact protein mass spectra were processed using MaxEnt1 or transform algorithms for charge deconvolution in the Mass-

Lynx 3.5 software (Micromass Ltd.). To identify peptide abundances of oxidized and reduced tryptic peptides of CaM_{ox}, samples were divided into two parts and desalted using either a hand-packed C_{18} trap column for analysis by electrospray ionization (ESI) or a ZipTip C_{18} (Millipore, Bedford, MA) for MALDI experiments. For ESI measurements, peptides were directly eluted from the trap column into the source of a Q-TOF2 mass spectrometer with 90:9.5:0.5 methanol/H_2O/formic acid (v/v/v) at 20 μL/min. Mass spectra were acquired in the *m*/*z* 300−2000 mass range at conditions optimized for peptide analysis. Charge deconvolution was performed using the MaxEnt3 module in the MassLynx 3.5 software (Micromass Ltd, UK). Intensities of ions corresponding to Met containing peptides and their oxiforms were measured to determine the kinetics of methionine sulfoxide repair. For MALDI measurements, peptides desalted on a ZipTip C_{18} were eluted on a stainless steel sample plate with a matrix consisting of 10 mg/mL of α-cyano-carboxycinnamic acid in 50.0:49.9:0.1 acetonitrile/H_2O/TFA (v/v/v). Mass spectra were acquired over *m*/*z* 700−4500 mass range using a Voyager-DE STR MALDI TOF mass spectrometer (PerSeptive Biosystems, Framingham, MA). The instrument was operated at conditions described in ref *45*. Ion intensities were taken for calculations after background subtract.

RESULTS

Prior measurements indicate that CaM_{ox}, which contains nine surface-exposed methionines (*46*), is a substrate for MsrA and MsrB. There is a large decrease in the helical structure of CaM upon oxidation of all nine methionines and a corresponding loss in the CaM-dependent activation of target proteins (*47*, *48*). Upon incubation with MsrA, CaM_{ox} assumes a native-like structure and fully recovers its function (*49*, *50*). To investigate the structural parameters that facilitate the recognition and reduction of Met(O) by MsrA in proteins, we measured the rates and extent of Met(O) reduction of CaM_{ox} by Msr following the quantitative oxidation of all nine methionines. We compared the extent of Met(O) reduction by MsrA in the intact protein with peptide fragments generated by exhaustive tryptic digestion, permitting a determination of how the protein fold affects the ability of MsrA to recognize Met(O) in proteins.

Incomplete Repair of S-Stereoisomer of Met(O) in CaM_{ox} by MsrA. We used ESI-MS to measure the mass of CaM. Prior to its oxidation by H_2O_2, the mass of CaM is 16 706.7 Da, consistent with the theoretical mass of 16 706.4 Da (Figure 1). A dehydration artifact associated with the ion trap results in the appearance of a lower molecular mass at 16 688.4 Da (*47*). Following oxidation with H_2O_2, the mass of CaM_{ox} is 16 850.0 Da; the 143.3 Da increase in mass indicates the quantitative oxidation of all nine methionines to their corresponding sulfoxides. Upon incubation with MsrA, there is a distribution of oxiforms, which contain between two and nine Met(O) per CaM. On average there are >6 Met(O) per CaM remaining after incubation with MsrA, indicating that approximately one-third of the oxidized methionines are reduced by MsrA. In contrast, upon incubation of intact CaM_{ox} with MsrBA, a bacterial fusion protein in which enzymes that selectively reduce both the S- and R-stereoisomers of Met(O) are within a single polypeptide chain and function to induce a more open protein structure,

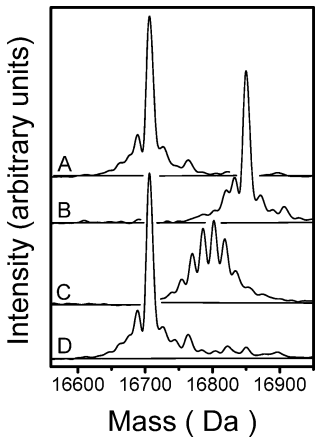

FIGURE 1: ESI-MS resolution of the distribution of CaM oxiforms corresponding to native CaM (A), CaM following the oxidation of all nine Met by H_2O_2 (B), or fully oxidized CaM following incubation with either MsrA (C) or MsrBA (D). Experimental conditions: 1.0 μM MsrA or MsrBA in the presence of 10 μM CaM_{ox} in 10 mM MOPS (pH 7.5), 50 mM KCl, and 15 mM DTT for 12 h at 25 °C.

one observes the nearly complete reduction of all Met(O) in CaM_{ox} (Figure 1). Because MsrA selectively reduces the S-stereoisomer of Met(O), which accounts for one-half of the oxidized methionines in CaM_{ox} (*51*), these results suggest that the formation of the native protein fold upon incubation of MsrA with CaM_{ox} may limit the ability of MsrA to recognize remaining Met(O). To investigate this possibility, we have disrupted the tertiary structure of CaM_{ox} through proteolytic digestion and measured the rates and extent of Met(O) reduction by MsrA.

We have used both ESI-MS and MALDI to measure the kinetics of Met(O) reduction following the incubation of MsrA with tryptic fragments derived from CaM_{ox}. There are large differences in the relative rates of Met(O) reduction within different peptides to repair by MsrA (Figure 2), suggesting that conformational restraints modulate the recognition of oxidized methionines by MsrA. Indeed, following tryptic digestion, rates of Met(O) reduction correlate inversely with the acidic charge density of the peptide (Figure 2B), which is consistent with the active site structure of MsrA that contains hydrophobic residues necessary for enzymatic activity (*31*). Significant fractions of each of the oxidized peptides remain, which correlates with the expected stochastic distribution of the R-stereoisomer of Met(O) in each peptide (Figure 2C) (*51*). A summation of the remaining Met(O) in each of the resolved peptides indicates that one-half of the Met(O) is reduced following incubation of MsrA with tryptic peptides of CaM_{ox} (Table 1). Thus, the incomplete repair of the intact CaM_{ox} by MsrA is the result of the protein-fold, consistent with prior measurements that demonstrated the MsrA-mediated repair of CaM_{ox} to induce a native secondary structure (*49*, *50*). Together, these results indicate that the recognition of Met(O) by MsrA in CaM_{ox} requires some disruption of the overall protein-fold.

Substrate Dependence of CaM_{ox} Repair. To assess whether Met(O) in CaM_{ox} can be reduced by MsrA at physiological concentrations, we measured the substrate-dependence of repair in the presence of saturating amounts of thioredoxin reductase and NADPH by varying the concentration of CaM_{ox}. The substrate-dependence of reductase activity can be described by simple Michaelis-Menton kinetics, where

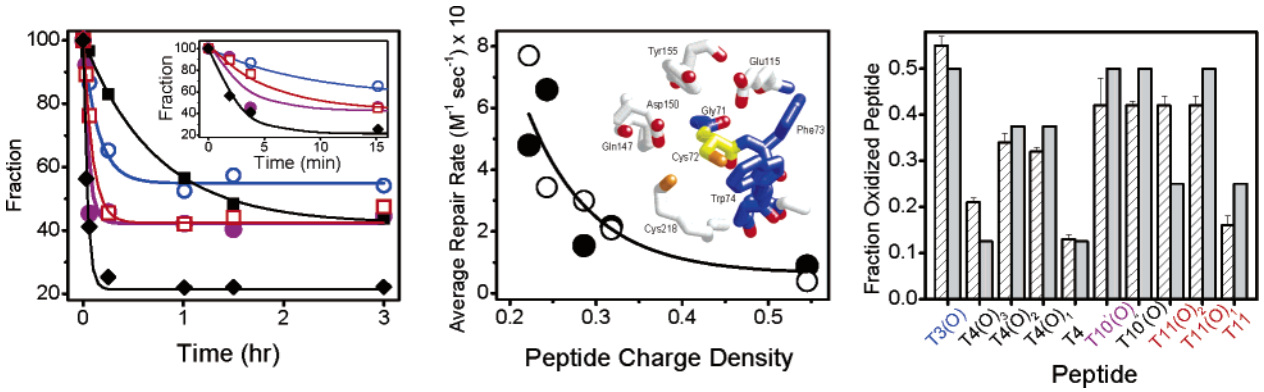

FIGURE 2: (A) Time-dependent reduction of tryptic peptides from CaM_{ox} measured using ESI-MS for peptide T3 (blue open circles), T4 (◆), T10′ (purple solid circles), T10″ (■), and T11 (red open squares) and (B) Relationship between rates of repair measured by ESI-MS (○) or MALDI (●) and peptide charge density, calculated as the fraction of charged amino acids in the sequence. Inset shows active site cysteine (yellow) and all amino acids within 5 Å, where hydrophobic amino acids are in blue, oxygens are red, and sulfurs are in orange. Tryptic peptides correspond to the following: T3, ELGTVMR; T4, SLGQNPTEAELQDMINEVDA DGNGTIDFPEFLTMMAR; T10′, HVMTLGEK; T10″, LTDEEVDEMIR; and T11, EADIDGDGQVNYEEF VQMMTAK. (C) Fraction of oxidized peptides following incubation with MsrA for 3 h (hatched) relative to the expected distribution of the R-stereoisomer of Met(O) assuming random oxidation (solid), where peptides are as indicated with the number of oxygens.

Table 1: ESI-MS Measurements of Rates and Extent of Met(O) Reduction in Tryptic Peptides of CaM_{ox}[a]

tryptic fragment[b]	observed monoisotopic mass[c] (Da)	theoretical mass[d] (Da)	sequence	rate[e] (M^{-1} s^{-1})	residual fraction[f]	Met(O) remaining[g]
T3(O)	820.4	820.4	E^{31}-Met^{36}-R^{37}	3000 (1700)	0.55 (0.02)	0.55 (0.02)
$T4(O)_3$	4116.8	4116.8	S^{38}-Met^{51}-Met^{71}-Met^{72}-R^{74}	10000 (2000)	0.21 (0.01)	0.63 (0.03)
$T4(O)_2$	4100.8	4100.8		12000 (8000)	0.34 (0.02)	0.68 (0.04)
T4(O)[h]	4084.9	4084.8		3500 (700)	0.32 (0.01)	0.32 (0.01)
T10′(O)	1043.5	1043.5	H^{107}-Met^{109}-K^{115}	8000 (5000)	0.42 (0.06)	0.42 (0.06)
T10″(O)	1364.6	1364.6	L^{116}-Met^{124}-R^{126}	400 (20)	0.42 (0.01)	0.42 (0.01)
$T11(O)_2$	2521.1	2521.1	E^{127}-Met^{144}-Met^{145}-K^{148}	3500 (400)	0.42 (0.02)	0.84 (0.03)
T11(O)[i]	2505.1	2505.1		4100 (50)	0.42 (0.02)	0.42 (0.02)

[a] All peptide ions were detected with an accuracy within 0.002% of the theoretical mass, and there were no ambiguities to the mass assignments of the peptide ions. [b] Nomenclature regarding the relationship between the peptides resulting from tryptic cleavage and the primary sequence of CaM is taken from Toda and co-workers (*80*). [c] ESI masses are measured and corrected for multiple charged forms. [d] Calculated masses are monoisotopic. [e] Apparent rate constants and standard deviations (in brackets) calculated from second-order rate equation, where the respective concentrations of MsrA and CaM peptides are 1.0 and 2.0 μM. [f] Residual Met(O) and standard deviations (in brackets) for each tryptic peptide following exhaustive repair. [g] Number of Met(O) remaining after exhaustive repair for resolved peptides containing a total of 8 Met(O) was 4.3 Met(O) per CaM (i.e., 3.7 Met per CaM were repaired). [h] Fraction of fully reduced T4 peptide remaining is 13 ± 1%. [i] Fraction of fully reduced T11 peptide remaining is 16 ± 2%. Tryptic peptide T7 containing Met^{76} was not resolved.

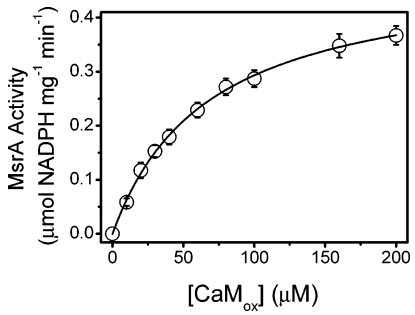

FIGURE 3: Substrate dependence of MsrA activity against CaM_{ox}, where experimental conditions involve 1 μM MsrA in 10 mM Tris-HCl (pH 7.5) in the presence of 2 μM thioredoxin reductase, 400 μM NADPH, and 50 μM thioredoxin at 24 °C. Line represents nonlinear least-squares fit to the Michaelis−Menton equation $V = (V_{max}[CaM_{ox}])/(K_M + [CaM_{ox}])$, where $K_M = 68 \pm 4$ μM and $V_{max} = 0.493 \pm 0.009$ μmol mg^{-1} min^{-1}.

K_M for CaM_{ox} is 68 ± 4 μM, with a maximal velocity of 0.493 ± 0.009 μmol mg^{-1} min^{-1} (Figure 3). Because neuronal CaM concentrations are near 60 μM (~1% of cellular protein) and essentially all CaM is oxidized during aging in some rat strains (*17*), these results indicate that MsrA has the potential to modulate the reduction of CaM_{ox} and other sensitive proteins (*52*). Furthermore, MsrA has a similar K_M using CaM_{ox} as a substrate in comparison to free Met-(O), where K_M is 33 μM (*31*). These results indicate that enzymatic turnover rates are not substantially affected by the binding sequence surrounding Met(O) and that the enzyme mechanism of the MsrA-dependent reduction of CaM_{ox} is similar to that of free Met(O), where the rate-limiting step occurs following the reduction of Met(O) and is associated with the thioredoxin-dependent reduction of MsrA (*29*).

High-Affinity Binding Between CaM_{ox} and MsrA. Under conditions of mild oxidative stress, the rates of Met(O) reduction are dependent on MsrA binding, while the subsequent dissociation of MsrA and its reduction by thioredoxin reductase may limit the overall rates of steady-state repair that becomes important under conditions of acute oxidative stress. However, current estimates that suggest relatively low-affinity binding between MsrA and oxidized methionines are derived primarily from kinetic measurements of the rates of free Met(O) reduction (*25*, *29*). There are no actual binding measurements to assess whether MsrA may play an important role in the recognition and repair of Met(O) in proteins,

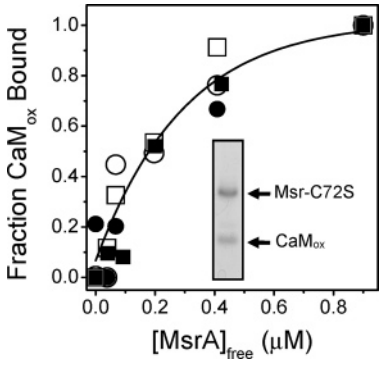

FIGURE 4: CaM_{ox} binding measured from fluorescence changes resulting from the association between Alexa532-labeled CaM_{ox} (0.1 μM) and MsrA were measured in 20 mM HEPES (pH 7.5), 100 mM KCl, 1.0 mM $MgCl_2$, 0.2 mM EGTA, in the absence (□, ■) or presence (○, ●) of 1.0 mM $CaCl_2$ for reduced (□, ○) or oxidized (■, ●) MsrA, where $\lambda_{ex} = 530$ nm and $\lambda_{em} = 580$ nm. Curve represents a nonlinear least-squares fit assuming a Langmuir binding isotherm, where $K_d = 250 \pm 50$ nM. Inset: SDS−PAGE of proteins following urea denaturation of complex between CaM_{ox} (10 μM) CaM_{ox} and MsrA (1.0 μM) that was affinity isolated using an immobilized antibody against the His-tag on MsrA using a Pierce ultralink Protein G resin and released by urea denaturation (6 M) following extensive washing.

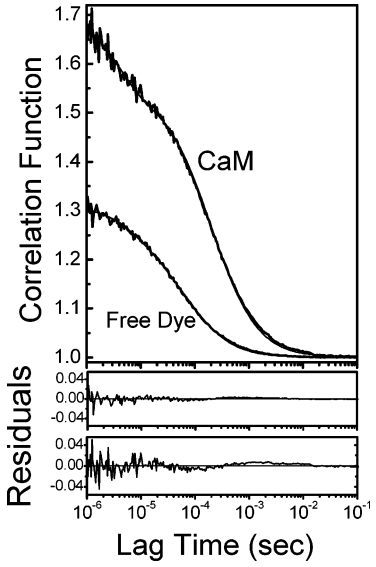

FIGURE 5: Fluorescence autocorrelation curves for Alexa532 alone (free dye) and covalently bound to CaM and associated nonlinear least-squares fits along with associated residuals for free dye (middle) and CaM (bottom) showing differences between experimental data and nonlinear least-squares fits. Experimental conditions involved 1 nM free dye or 5 nM CaM in 10 mM MOPS (pH 7.0) and 50 mM KCl.

preventing a mechanistic understanding of whether the accumulation of Met(O) in CaM during biological aging arises because of increased rates of ROS generation, diminished thioredoxin levels, or an inability of MsrA to bind and reduce modest amounts of oxidative damage (*7*, *17*). To measure the binding interaction between MsrA and CaM_{ox}, we used site-directed mutagenesis to substitute the active site cysteine (i.e., Cys^{72}) with serine to functionally inactivate the enzyme. The mutant enzyme (i.e., MsrA-C72S) retains proximal cysteines (i.e., Cys^{218} and Cys^{227}) that are reduced by thioredoxin reductase and function as part of a redox shuttle in promoting MsrA catalysis (*9*, *10*). Following the covalent attachment of the fluorophore Alexa532 onto CaM_{ox}, there is a 50% increase in fluorescence upon association of Alexa532-CaM_{ox} with MsrA-C72S, which reflects the binding of CaM_{ox} by MsrA, as demonstrated by their co-immunoprecipitation (see inset in Figure 4). Upon titration with MsrA-C72S, one observes substantial binding, with a half-point of the titration near 200 nM for both apo- and calcium-activated CaM (Figure 4). Furthermore, similar binding curves are observed irrespective of whether MsrA is in a reduced or oxidized state, indicating that there are no large changes around the active site of MsrA that modulate binding. These results demonstrate a high-affinity binding interaction between MsrA and CaM_{ox} and suggest that MsrA can reduce low levels of Met(O) in CaM_{ox} to modulate protein function. However, while these results indicate a high-affinity association between CaM_{ox} and MsrA, they are unable to account for multisite binding in which multiple MsrA proteins may associate with each CaM_{ox}. In contrast, fluorescence correlation spectroscopy (FCS) provides the resolution to distinguish the relative populations of unbound CaM from that associating with MsrA bound to CaM by their changes in size or diffusion coefficients (see below).

Relationship Between Protein Size and Translational Diffusion Coefficient. High-affinity interactions between proteins are optimally measured using single-molecule methods such as fluorescence correlation spectroscopy (FCS), which permits the determination of the size of the protein complex through the direct measurement of the translational diffusion coefficient (D_t). Using FCS, we measured the autocorrelation curves for the free dye Alexa532 and following its covalent binding to CaM (Figure 5). Optimal nonlinear least-squares fits to the data involved a model with one triplet state and one diffusion component, which resulted in excellent fits as evidenced by the essentially random residuals. In the case of the free dye, the triplet lifetime and diffusion times were 7.7 ± 0.8 μs and 64 ± 1.5 μs, respectively, with amplitudes of 16 and 84%. From the mass, we can calculate that $D_t = 3.3 \times 10^{-10}$ m^2 s^{-1} for Alexa532, which is in excellent agreement with the measured value (i.e., $D_t = 3.2 \times 10^{-10}$ m^2 s^{-1}). Likewise, the triplet lifetime and diffusion time for Alexa532-labeled CaM was 3.8 ± 0.2 μs and 199 ± 2 μs with amplitudes of 23 and 77%. The corresponding diffusion coefficient is 1.0×10^{-10} m^2 s^{-1}, which is in close agreement with the theoretical value of 0.9×10^{-10} m^2 s^{-1} for calcium-activated CaM calculated from the crystal structure 1cll.pdb using the program Hydropro (*53*). Upon binding a CaM-specific antibody the diffusion time calculated for Alexa532-labeled CaM increases to 282 μs (data not shown), emphasizing the sensitivity of measurements of translational diffusion to the size of the protein complex.

Quantitative Determination of Binding Affinity and Stoichiometry Between MsrA and CaM_{ox}. From a consideration of the correlation functions for Alexa532-labeled CaM as a function of increasing concentrations of MsrA-C72S, one can measure the binding affinity and stoichiometry. Increases in the concentration of MsrA-C72S result in progressive shifts in the correlation function of Alexa532-labeled CaM_{ox} toward longer lag times, which indicate a larger protein complex (Figure 6A). In comparison, there is no shift in the correlation function of fully reduced CaM in the presence of MsrA-C72S (Figure 7), indicating that in the absence of oxidation CaM does not associate with MsrA. In these binding measurements, the concentration of CaM_{ox} is so

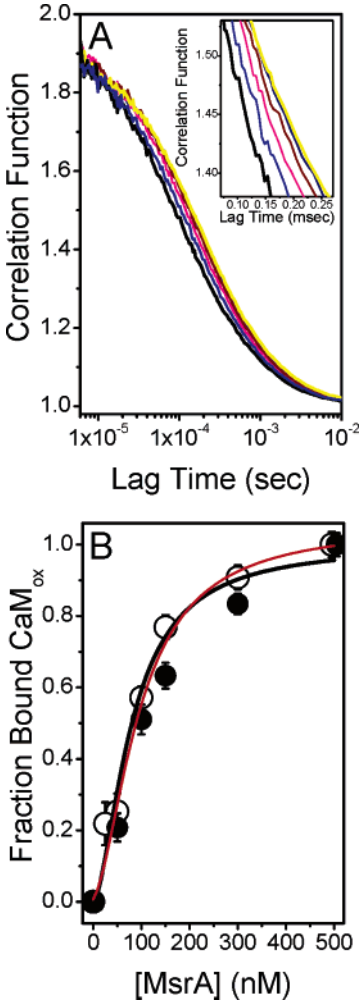

FIGURE 6: (A) Fluorescence autocorrelation curves and midpoint (see inset) for Alexa532-labeled CaM_{ox} (5 nM) in the presence of variable concentrations of reduced MsrA-C72S, which varies from 0 nM (black), 50 nM (royal blue), 100 nM (pink), 150 nM (brown), 300 nM (navy blue), and 500 nM (yellow). Experimental conditions involve 20 mM HEPES (pH 7.5), 100 mM KCl, 1.0 mM $MgCl_2$, 0.2 mM EGTA, 1 mM $CaCl_2$, and 15 mM DTT at 20 °C. (B) Fraction of CaM_{ox} bound to reduced (○) or oxidized (●) MsrA-C72S, where fraction of bound CaM_{ox} corresponds to $(1 - \alpha)$ in eq 1 in Experimental Procedures. Curves represent nonlinear least-squares fit to the Hill eqn (eq 5, black curve) ($K = 70 \pm 10$ nM; $n = 1.7 \pm 0.2$) or a model involving homotropic cooperativity (eq 7, red curve) ($\Delta G_1 = -9.0 \pm 0.2$ kcal/mol; $\Delta G_2 = -19.13 \pm 0.05$ kcal/mol; $\Delta G_c = -1.9 \pm 0.2$ kcal/mol).

small (i.e., 5 nM) that binding has essentially no effect on the concentration of free (unbound) MsrA. There are progressively smaller shifts in the correlation function upon addition of MsrA-C72S, whereby essentially overlapping curves are observed upon addition of 300 and 500 nM MsrA-C72S. Under saturating conditions, the correlation function can be readily fit to a simple model to determine the diffusion time, which was 231 ± 3 μs, corresponding to a diffusion coefficient of $0.86 \pm 0.01 \times 10^{-10}$ m^2 s^{-1}. The 16% decrease in the translational diffusion coefficient permits an estimate of the size of the protein complex, which has an apparent mass of ~75 kDa, suggesting a complex involving two MsrA proteins bound to each CaM_{ox}. This calculation assumes that both CaM and its bound complex with MsrA have the same overall shape, such that changes in the translational diffusion coefficient are directly related to changes in the mass of the complex. The error in the calculated radius is likely to be

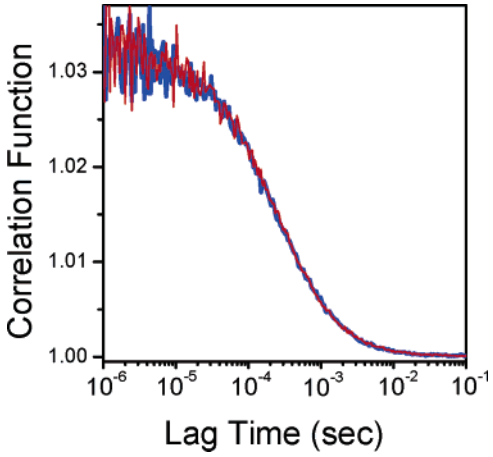

FIGURE 7: Fluorescence autocorrelation curves for Alexa488-labeled CaM (90 nM), in which all methionines are fully reduced, in the absence (red curve) and presence (blue curve) of 1.0 μM MsrA-C72S. Experimental conditions are as described in the legend to Figure 6.

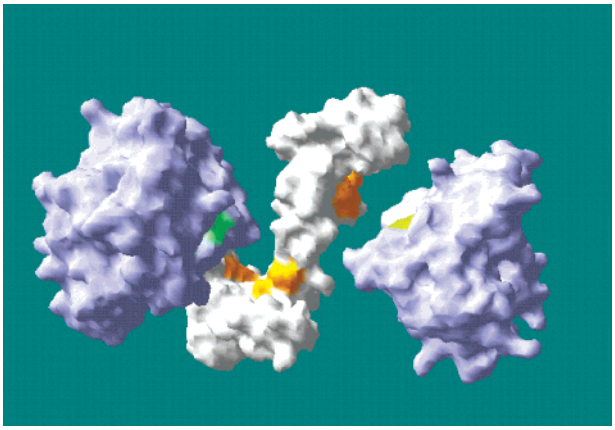

FIGURE 8: Cartoon showing structural arrangement of Met(O) (orange) in CaM_{ox} (white) relative to active site region Gly^{71}-Cys-Phe-Trp-Gly^{75} (green) of MsrA (purple), where clusters of methionines are respectively located in the amino-domain (i.e., Met^{36}, Met^{51}, Met^{71}, Met^{72}, and Met^{76}) or the carboxyl-terminal domain (Met^{109}, Met^{124}, Met^{144}, and Met^{145}). Structures correspond to 1cll.pdb (CaM) or 1fva.pdb (MsrA) (*10*, *81*), and are drawn using the Swiss-pdb viewer program (*82*).

no more than about 5%, since a 2-fold change in the axial ratio of the particle results in a 4.4 and 4.2% changes in the frictional coefficient for a prolate and oblate ellipsoid (*54*), suggesting an error of about 12 kDa in the estimated mass of the complex. Thus, the calculated mass of 75 kDa is indicative of a complex involving one CaM and two bound MsrA (i.e., 17 + 23 + 23 kDa = 63 kDa), as opposed to CaM bound to a single MsrA (40 kDa) or three MsrA (98 kDa). This latter conclusion is, furthermore, consistent with the structure of CaM, which contains nine methionines located in two spatially distinct clusters; one in each domain (Figure 8). Indeed, considering the structure of MsrA, whose active site is highlighted, it is apparent that steric constraints limit the binding of one MsrA to each domain of CaM.

Additional resolution of the binding interaction between MsrA and CaM_{ox} was obtained from a consideration of all FCS correlation curves, which were simultaneously fit assuming a linear combination of the diffusion times associated with unbound Alexa532-labeled CaM_{ox} (i.e., 199 ± 2 μs) and the MsrA-C72S bound complex (231 ± 3 μs) (see

eq 1 in Experimental Procedures) to determine the fraction of bound CaM_{ox} (Figure 6B), which is independent of assumptions of the overall shape of CaM or its complex with MsrA. Similar binding curves are observed irrespective of whether redox cycling cysteines in MsrA-C72S were oxidized or reduced, indicating that the specificity of binding is independent of the redox state of MsrA. The binding affinity determined using the Hill equation indicates that $K = 70 \pm 10$ nM; the Hill coefficient ($n = 1.7 \pm 0.2$) indicates the cooperative binding of two MsrA to each CaM. Since binding is cooperative, K is the sum of the two microscopic equilibrium dissociation constants for binding each of the MsrA proteins to CaM, i.e., $K = k_1 + k_2$ (i.e., homotropic cooperativity) (*43*). An explicit consideration of this model permits a lower estimation of the cooperative binding interaction (*44*) and suggests that the free energy associated with cooperative binding is about 2 kcal/mol (see legend of Figure 6B). These latter results suggest that the association of one MsrA promotes the structural recognition of the second MsrA, which may involve either the stabilization of CaM_{ox} in a partially unfolded conformation to enhance MsrA binding or some productive binding interaction between multiple MsrA that facilitates their recruitment to associate with CaM_{ox}.

DISCUSSION

We demonstrated the cooperative and high-affinity binding of multiple MsrA to CaM_{ox} ($K = 70 \pm 10$ nM) that reduces the S-stereoisomer of Met(O) within highly accessible sequences (Figures 2 and 6). The majority of S-stereoisomers of Met(O) are repaired, resulting in the restoration of a native protein fold and CaM_{ox} function (*49*, *50*). However, significant amounts of the S-stereoisomer of Met(O) remain that are not substrates for further reduction by MsrA, despite their significant surface accessibilities (Figures 1 and 9). In contrast, following tryptic digestion, there is a full reduction of all of the S-stereoisomers of Met(O) by MsrA (Figure 2), indicating that surface-exposed S-stereoisomers of Met(O) within folded proteins need not be substrates for MsrA. These latter results contrast with those of Grimaud and co-workers who reported the complete repair of all S-Met(O) by MsrA in CaM (*25*). However, these earlier MALDI measurements lacked the resolution to fully resolve all oxidized methionines and reported the reduction of more than 60% of Met(O) in CaM_{ox} using either MsrA or MsrB alone (*25*). In contrast, we report that MsrA reduced <35% of Met(O) in CaM_{ox}, while half of the Met(O) is reduced (i.e., virtually all of the S-stereoisomer) following tryptic digestion. Moreover, a fusion protein obtained from pathogenic bacteria that can reduce both stereoisomers (MsrBA) fully reduces all oxidized methionines (Figure 1), confirming that the observed retention of >65% of Met(O) in CaM_{ox} is not the result of incomplete repair of the S-Met(O) by MsrA. Together, these results suggest that the oxidant-induced disruption of protein structure enhances the ability of Msr to bind and reduce Met(O).

Oxidant-induced structural unfolding may facilitate recognition and repair of Met(O) by enhancing access to the active site cysteine (C72) in MsrA, whose limited surface accessibility precludes the recognition of highly structured and surface-inaccessible sequences. Indeed, a consideration of the structure solved by Lowther and colleagues (*10*) indicates the active site cysteine has a relatively small surface accessibility, whose sulfur is not accessible to sites with an effective radius larger than 4 Å [calculated using 1FVG.pdb and the program Surface Racer 1.1 (*55*)]. Given the additional steric restriction associated with binding Met(O) within folded proteins, these observations are consistent with an inability of MsrA to reduce the majority of Met(O) in a wide range of different proteins, which make up between 4−9% of all methionines (*7*). However, regardless of the mechanism, the observation that there is essentially complete repair of the S-stereoisomer of Met(O) by MsrA only following proteolytic digestion indicates that the disruption of the overall protein fold is necessary for recognition and repair of Met(O) by MsrA. These findings suggest that the ability of MsrA to recognize and repair Met(O) within disordered sequences regulates the function of a subset of proteins that are conformationally sensitive to oxidative stress.

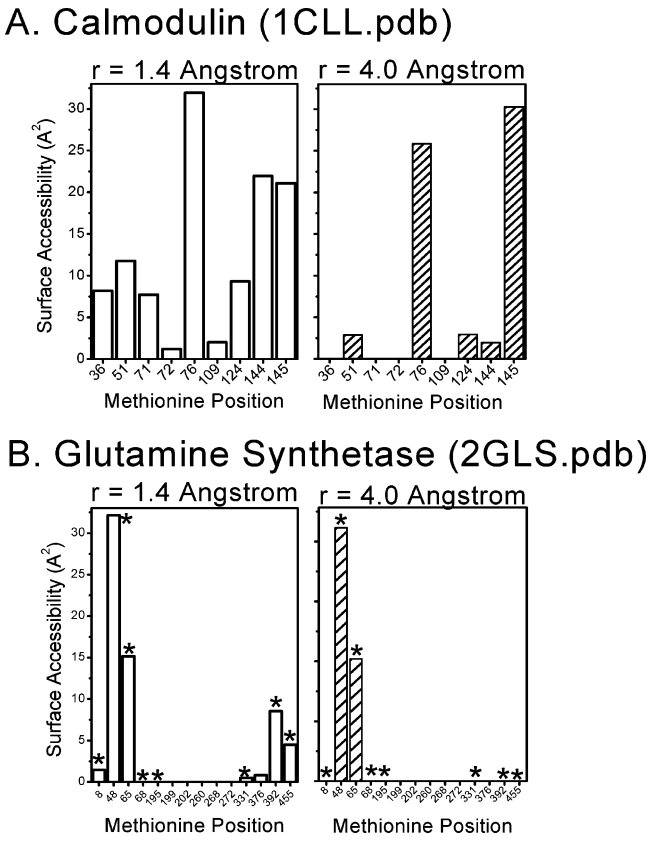

FIGURE 9: Surface accessibilities of methionines in calmodulin (1cll.pdb) and glutamine synthetase (2gls.pdb) to a sphere of the indicated radii were calculated using the program Surface Racer 1.1 (*55*), assuming a radius of either 1.4 Å (left panels; approximate radii of hydrogen peroxide) or 4.0 Å (right panels; estimated to be an accessible surface area of active site sulfur C72 in 1FVG.pdb to protein associated methionine sulfoxides). In the case of glutamine synthetase, sites demonstrated to be selectively oxidized by hydrogen peroxide are indicated by an asterisk (∗) (*69*).

MsrA and Met(O) Reduction. Prior measurements have demonstrated that multiple Msr are present in all cell types, suggesting a universal requirement for maintaining some or all Met(O) in a reduced state. Two classes of Msr enzymes (i.e., A and B) with mirror-image active sites function to specifically reduce the S- and R-stereoisomers of either free or protein-bound Met(O) (*9*, *10*, *25*, *30*, *56*). The maintenance of free methionine necessary for amino-acyl tRNA charging for the initiation of protein synthesis or in the biosynthesis

of S-adenosylmethionine may represent primary functions of Msr. Consistent with this suggestion, the K_M of bovine Msr for free Met(O) is 33 μM (*31*), which is substantially less than the 400 μM concentration of the free amino acid methionine in cells (Human Metabolite Database; http://metabolibrary.ca/). In addition, it has been suggested that Msr plays a general role in repair and refolding of oxidized proteins to modulate cell function (*1*, *2*, *57*). Consistent with the latter suggestion, we find that methionine sulfoxides within uncharged and hydrophobic protein sequences of CaM_{ox} are selectively reduced (Figure 2B). These results are consistent with the hydrophobic active site and structural data indicating the stabilization of the terminal methyl of the Met(O) by a hydrophobic side chain interaction involving a conserved tryptophan is necessary for catalytic reduction of Met(O) (Figure 2B) (*58*).

Binding and reduction of Met(O) is an order of magnitude larger for MsrA than MsrB (*29*), suggesting the preferential reduction of the S-stereoisomer of Met(O) in cells under conditions of oxidative stress that may relate to differential stereochemical modifications by different reactive oxygen species (*59*). The physiological consequences of the preferential reduction of the S-stereoisomer of Met(O) is apparent from a consideration of CaM, whose nine surface-exposed methionines serve as a model system to understand the structural requirements associated with the recognition and repair of Met(O) by MsrA or MsrB (*25*, *51*, *59*). For example, the site-specific oxidation of $Met(O)^{144}$/$Met(O)^{145}$ in CaM results in large tertiary structural changes of CaM that allow repair by MsrA and degradation by the 20S proteasome (*47*, *49*, *50*, *60*−*63*). The MsrA-dependent reduction of the S-stereoisomer in CaM results in both the full restoration of function and the normal protein fold (*49*, *50*), suggesting that stereospecific oxidation of Met to form S-Met(O) regulates CaM function. This is important because while hydrogen peroxide results in equimolar distributions of the S- and R-stereoisomers of Met(O), other reactive oxygen species (e.g., peroxy radicals) can exhibit a stereoselective oxidation of methionines to preferentially form either the S- or R-stereoisomer (*59*).

Aging and Methionine Sulfoxide Formation. Increases in Met(O) content in cellular lysates have been observed in response to conditions of oxidative stress and have been linked to the loss of specific protein functions during aging (*1*). Consistent with this latter suggestion, protein abundances of Msr decline during aging (*64*) and may contribute to age-dependent declines in cellular function and the accumulation of functionally inactive CaM in some rodent strains (*17*, *65*). Indeed, age-dependent increases in the levels of Met(O) in CaM isolated from both mouse and rat brains have been observed, which results in a diminished transport activity of CaM-dependent calcium pumps and channels (*17*, *65*−*67*). Nevertheless, there are no global increases in the abundances of Met(O) in cellular brain lysates during biological aging (*7*). Furthermore, in agreement with the observation by Schöneich that the oxidation of calmodulin need not occur in all strains of rats (*7*), CaM isolated from long-lived rodent strains is not oxidized in unstressed aged animals (*18*). These latter results suggest that the ability to maintain reduced CaM may contribute to healthy aging.

An understanding of the mechanisms that underlie the accumulation of Met(O) in young animals is apparent from our data concerning the MsrA-dependent reduction of CaM_{ox}, whose oxidation can be physiologically important during aging and serves as a model system to understand the substrate requirements associated with protein repair by MsrA. This follows from the fact that all methionines in calcium-activated CaM are surface exposed and are thus readily oxidized by small molecules (such as hydrogen peroxide or peroxynitrite) (Figure 9). However, steric effects associated with the active site geometry and protein fold of MsrA limit the ability to recognize and reduce S-stereoisoforms of Met(O) in folded proteins, consistent with the retention of Met(O) in CaM_{ox} and other proteins (*7*). Following the proteolytic digestion of CaM_{ox} all S-stereoisomers of Met(O) are fully reduced (Figure 2), suggesting that surface-exposed Met(O) within unstructured protein sequences are substrates for MsrA. In contrast, the majority of methionines are excluded from the surface of proteins (*68*) such that when oxidized [for example, see Met^{68} and Met^{195} in glutamine synthetase; 2GLS.pdb (*69*)] (see Figure 9) they are inaccessible to the active site of MsrA. These prior measurements suggest that some methionines that are sufficiently exposed to serve as antioxidant sinks for reactive oxygen species may not be substrates for Msr due to steric constraints associated with the protein fold.

A subset of conformationally sensitive proteins, including CaM, represent sensors whose oxidation modulates intracellular signaling (*1*). Indeed, global structural changes following the oxidation of Met^{144} or Met^{145} in CaM result in its nonproductive interaction with some target proteins, including the plasma membrane Ca-ATPase, to modulate calcium resequestration to prolong the calcium transient and diminish energy use under conditions of oxidative stress (*17*, *47*, *48*, *60*, *61*, *70*). Likewise, methionine oxidation has been reported to modulate the function of a number of other proteins, including α_1-protease inhibitor, high-mobility-group protein HMG-D, chymotrypsin, thrombomodulin, and calcium-activated potassium channels (*71*−*73*). In contrast, less accessible methionines can function as antioxidant sinks that protect active sites, as in glutamine synthetase (*69*). In this latter case, methionines have been suggested to line the pocket leading to an active site metal and preserve protein function (*74*). Thus, methionines can serve both antioxidant and regulatory roles, maintaining protein activity or as part of an adaptive cellular response to acute conditions of oxidative stress.

Conclusions and Future Directions. We have demonstrated the cooperative and high-affinity binding of CaM_{ox} by MsrA. Reduction Met(O) by MsrA is facilitated by a disruption of the protein fold following proteolytic digestion, consistent with conformational restrictions associated with the active site of MsrA. These observations are consistent with the inability of MsrA to repair surface-accessible S-stereoisomers of Met(O) in CaM_{ox} following restoration of the native protein fold (*75*). Oxidation of the vast majority of methionines has essentially no effect on the structure of CaM (*61*), indicating that even in a metastable protein such as CaM that Met(O) formation does not as a rule affect the global fold. Rather, the oxidation of specific Mets in CaM (i.e., Met^{144} and Met^{145}) destabilizes the C-terminus helix to induce global conformational changes (*48*, *61*, *76*−*79*). These results suggest that MsrA selectively recognizes Met(O) following the introduction of oxidant-induced conformational disorder

and that MsrA may function to modulate the functions of a subset of proteins in a redox-dependent manner. Future measurements should focus on identifying this family of protein sensors and measuring time-dependent changes in their oxidation to uncover inherent regulatory strategies that modulate cell function.

ACKNOWLEDGMENT

We wish to thank Diana J. Bigelow, Leslie B. Poole, and Jeffrey L. Urbauer for insightful discussions and Julie Gephardt for technical editing.

REFERENCES

1. Bigelow, D. J., and Squier, T. C. (2005) Redox modulation of cellular signaling and metabolism through reversible oxidation of methionine sensors in calcium regulatory proteins, *Biochim. Biophys. Acta (BBA) − Proteins Proteomics 1703*, 121−134.
2. Vogt, W. (1995) Oxidation of methionyl residues in proteins: tools, targets, and reversal, *Free Radic. Biol. Med. 18*, 93−105.
3. Dalle-Donne, I., Rossi, R., Ceciliani, F., Giustarini, D., Colombo, R., and Milzani, A. (2006) *Proteins as Sensitive Biomarkers of Human Conditions Associated with Oxidative Stress; Redox Proteomics: From Protein Modifications to Cellular Dysfunction and Diseases*, John Wiley & Sons, Hoboken, New Jersey.
4. Alvarez, B., Ferrer-Sueta, G., Freeman, B. A., and Radi, R. (1999) Kinetics of peroxynitrite reaction with amino acids and human serum albumin, *J. Biol. Chem. 274*, 842−848.
5. Berlett, B. S., and Stadtman, E. R. (1997) Protein oxidation in aging, disease, and oxidative stress, *J. Biol. Chem. 272*, 20313−20316.
6. Midwinter, R. G., Cheah, F. C., Moskovitz, J., Vissers, M. C., and Winterbourn, C. C. (2006) IkappaB is a sensitive target for oxidation by cell-permeable chloramines: inhibition of NF-kappaB activity by glycine chloramine through methionine oxidation, *Biochem. J. 396*, 71−78.
7. Stadtman, E. R., Van Remmen, H., Richardson, A., Wehr, N. B., and Levine, R. L. (2005) Methionine oxidation and aging, *Biochim. Biophys. Acta. 1703*, 135−140.
8. Weissbach, H., Resnick, L., and Brot, N. (2005) Methionine sulfoxide reductases: history and cellular role in protecting against oxidative damage, *Biochim. Biophys. Acta (BBA) − Proteins Proteomics 1703*, 203−212.
9. Lowther, W. T., Brot, N., Weissbach, H., Honek, J. F., and Matthews, B. W. (2000) Thiol-disulfide exchange is involved in the catalytic mechanism of peptide methionine sulfoxide reductase, *Proc. Natl. Acad. Sci. U.S.A. 97*, 6463−6468.
10. Lowther, W. T., Brot, N., Weissbach, H., and Matthews, B. W. (2000) Structure and mechanism of peptide methionine sulfoxide reductase, an "anti-oxidation" enzyme, *Biochemistry 39*, 13307−13312.
11. Bernstein, H. D., Poritz, M. A., Strub, K., Hoben, P. J., Brenner, S., and Walter, P. (1989) Model for signal sequence recognition from amino-acid sequence of 54K subunit of signal recognition particle, *Nature 340*, 482−486.
12. O'Neil, K. T., and DeGrado, W. F. (1990) How calmodulin binds its targets: sequence independent recognition of amphiphilic alpha-helices, *Trends Biochem. Sci. 15*, 59−64.
13. O'Neil, K. T., Erickson-Viitanen, S., and DeGrado, W. F. (1989) Photolabeling of calmodulin with basic, amphiphilic alpha-helical peptides containing *p*-benzoylphenylalanine, *J. Biol. Chem. 264*, 14571−14578.
14. Gellman, S. H. (1991) On the role of methionine residues in the sequence-independent recognition of nonpolar protein surfaces, *Biochemistry 30*, 6633−6636.
15. Yan, P., Xiong, Y., Chen, B., Negash, S., Squier, T. C., and Mayer, M. U. (2006) Fluorophore-assisted light inactivation of calmodulin involves singlet-oxygen mediated cross-linking and methionine oxidation, *Biochemistry 45*, 4736−4748.
16. Hoshi, T., and Heinemann, S. H. (2001) Regulation of cell function by methionine oxidation and reduction, *J. Physiol. (London) 531*, 1−11.
17. Gao, J., Yin, D., Yao, Y., Williams, T. D., and Squier, T. C. (1998) Progressive decline in the ability of calmodulin isolated from aged brain to activate the plasma membrane Ca-ATPase, *Biochemistry 37*, 9536−9548.
18. Zaidi, A., Gao, J., Squier, T. C., and Michaelis, M. L. (1998) Age-related decrease in brain synaptic membrane Ca2+-ATPase in F344/BNF1 rats, *Neurobiol. Aging 19*, 487−495.
19. Moskovitz, J., Bar-Noy, S., Williams, W. M., Requena, J., Berlett, B. S., and Stadtman, E. R. (2001) Methionine sulfoxide reductase (MsrA) is a regulator of antioxidant defense and lifespan in mammals, *Proc. Natl. Acad. Sci. U.S.A. 98*, 12920−12925.
20. Ruan, H., Tang, X. D., Chen, M. L., Joiner, M. L., Sun, G., Brot, N., Weissbach, H., Heinemann, S. H., Iverson, L., Wu, C. F., and Hoshi, T. (2002) High-quality life extension by the enzyme peptide methionine sulfoxide reductase, *Proc. Natl. Acad. Sci. U.S.A. 99*, 2748−2753.
21. Gabbita, S. P., Aksenov, M. Y., Lovell, M. A., and Markesbery, W. R. (1999) Decrease in peptide methionine sulfoxide reductase in Alzheimer's disease brain. *J. Neurochem. 73*, 1660−1666.
22. Glaser, C. B., Yamin, G., Uversky, V. N., and Fink, A. L. (2005) Methionine oxidation, alpha-synuclein and Parkinson's disease, *Biochim. Biophys. Acta 1703*, 157−169.
23. Hokenson, M. J., Uversky, V. N., Goers, J., Yamin, G., Munishkina, L. A., and Fink, A. L. (2004) Role of individual methionines in the fibrillation of methionine-oxidized alpha-synuclein, *Biochemistry 43*, 4621−4633.
24. Krishnan, S., Chi, E. Y., Wood, S. J., Kendrick, B. S., Li, C., Garzon-Rodriguez, W., Wypych, J., Randolph, T. W., Narhi, L. O., Biere, A. L., Citron, M., and Carpenter, J. F. (2003) Oxidative dimer formation is the critical rate-limiting step for Parkinson's disease alpha-synuclein fibrillogenesis, *Biochemistry 42*, 829−837.
25. Grimaud, R., Ezraty, B., Mitchell, J. K., Lafitte, D., Briand, C., Derrick, P. J., and Barras, F. (2001) Repair of Oxidized Proteins. Identification of a new methionine sulfoxide reductase, *J. Biol. Chem. 276*, 48915−48920.
26. Hansel, A., Heinemann, S. H., and Hoshi, T. (2005) Heterogeneity and function of mammalian MSRs: enzymes for repair, protection and regulation, *Biochim. Biophys. Acta 1703*, 239−247.
27. Boschi-Muller, S., Azza, S., and Branlant, G. (2001) E. coli methionine sulfoxide reductase with a truncated N terminus or C terminus, or both, retains the ability to reduce methionine sulfoxide, *Protein Sci. 10*, 2272−2279.
28. Weissbach, H., Etienne, F., Hoshi, T., Heinemann, S. H., Lowther, W. T., Matthews, B., St. John, G., Nathan, C., and Brot, N. (2002) Peptide methionine sulfoxide reductase: structure, mechanism of action, and biological function, *Arch. Biochem. Biophys. 397*, 172−178.
29. Boschi-Muller, S., Olry, A., Antoine, M., and Branlant, G. (2005) The enzymology and biochemistry of methionine sulfoxide reductases. *Biochim. Biophys. Acta (BBA) − Proteins Proteomics 1703*, 231−238.
30. Brot, N., and Weissbach, H. (2000) Peptide methionine sulfoxide reductase: Biochemistry and physiological role, *Peptide Sci. 55*, 288−296.
31. Moskovitz, J., Poston, J. M., Berlett, B. S., Nosworthy, N. J., Szczepanowski, R., and Stadtman, E. R. (2000) Identification and characterization of a putative active site for peptide methionine sulfoxide reductase (MsrA) and its substrate stereospecificity, *J. Biol. Chem. 275*, 14167−14172.
32. Nelson, D. P., and Kiesow, L. A. (1972) Enthalpy of decomposition of hydrogen peroxide by catalase at 25 degrees C (with molar extinction coefficients of H_2O_2 solutions in the UV), *Anal. Biochem. 49*, 474−478.
33. Huhmer, A. F., Gerber, N. C., de Montellano, P. R., and Schoneich, C. (1996) Peroxynitrite reduction of calmodulin stimulation of neuronal nitric oxide synthase, *Chem. Res. Toxicol. 9*, 484−491.
34. Strasburg, G. M., Hogan, M., Birmachu, W., Thomas, D. D., and Louis, C. F. (1988) Site-specific derivatives of wheat germ calmodulin. Interactions with troponin and sarcoplasmic reticulum, *J. Biol. Chem. 263*, 542−548.
35. Moskovitz, J., Weissbach, H., and Brot, N. (1996) Cloning the expression of a mammalian gene involved in the reduction of methionine sulfoxide residues in proteins, *Proc. Natl. Acad. Sci. U.S.A. 93*, 2095−2099.
36. Sambrook, J., Fritsch, E. F., and Maniatis, T. (1989) *Molecular Cloning: A Laboratory Manual*, 2nd ed., Cold Spring Harbor Laboratory Press, Cold Spring Harbor, NY.

37. Hemsley, A., Arnheim, N., Toney, M. D., Cortopassi, G., and Galas, D. J. (1989) A simple method for site-directed mutagenesis using the polymerase chain reaction, *Nucleic Acids Res. 17*, 6545−6551.
38. Weiner, M. P., Costa, G. L., Schoettlin, W., Cline, J., Mathur, E., and Bauer, J. C. (1994) Site-directed mutagenesis of double-stranded DNA by the polymerase chain reaction, *Gene 151*, 119−123.
39. Rutberg, B., and Hoch, J. A. (1970) Citric acid cycle: gene-enzyme relationships in *Bacillus subtilis*, *J. Bacteriol. 104*, 826−833.
40. Gillespie, P. G., and Cyr, J. L. (2002) Calmodulin binding to recombinant myosin-1c and myosin-1c IQ peptides, *BMC Biochem. 3*, 31.
41. Reddy, V. S., Safadi, F., Zielinski, R. E., and Reddy, A. S. (1999) Interaction of a kinesin-like protein with calmodulin isoforms from Arabidopsis, *J. Biol. Chem. 274*, 31727−31733.
42. Magde, D., Elson, E. L., and Webb, W. W. (1974) Fluorescence correlation spectroscopy. II. An experimental realization, *Biopolymers 13*, 29−61.
43. Matthews, J. C. (1993) *Fundamentals of Receptor, Enzyme, and Transport Kinetics*; pp 50−54, CRC Press, Boca Raton.
44. Pedigo, S., and Shea, M. A. (1995) Quantitative endoproteinase GluC footprinting of cooperative Ca2+ binding to calmodulin: proteolytic susceptibility of E31 and E87 indicates interdomain interactions, *Biochemistry 34*, 1179−1196.
45. Galeva, N., and Altermann, M. (2002) Comparison of one-dimensional and two-dimensional gel electrophoresis as a separation tool for proteomic analysis of rat liver microsomes: cytochromes P450 and other membrane proteins, *Proteomics 2*, 713−722.
46. Babu, Y. S., Bugg, C. E., and Cook, W. J. (1988) Structure of calmodulin refined at 2.2 Å resolution, *J. Mol. Biol. 204*, 191−204.
47. Gao, J., Yin, D. H., Yao, Y., Sun, H., Qin, Z., Schoneich, C., Williams, T. D., and Squier, T. C. (1998) Loss of conformational stability in calmodulin upon methionine oxidation, *Biophys. J. 74*, 1115−1134.
48. Bartlett, R. K., Bieber Urbauer, R. J., Anbanandam, A., Smallwood, H. S., Urbauer, J. L., and Squier, T. C. (2003) Oxidation of Met144 and Met145 in calmodulin blocks calmodulin dependent activation of the plasma membrane Ca-ATPase, *Biochemistry 42*, 3231−3238.
49. Sun, H., Gao, J., Ferrington, D. A., Biesiada, H., Williams, T. D., and Squier, T. C. (1999) Repair of oxidized calmodulin by methionine sulfoxide reductase restores ability to activate the plasma membrane Ca-ATPase, *Biochemistry 38*, 105−112.
50. Ferrington, D. A., Sun, H., Murray, K. K., Costa, J., Williams, T. D., Bigelow, D. J., and Squier, T. C. (2001) Selective degradation of oxidized calmodulin by the 20 S proteasome, *J. Biol. Chem. 276*, 937−943.
51. Sharov, V. S., Ferrington, D. A., Squier, T. C., and Schoneich, C. (1999) Diastereoselective reduction of protein-bound methionine sulfoxide by methionine sulfoxide reductase, *FEBS Lett. 455*, 247−250.
52. Halvey, P. J., Watson, W. H., Hansen, J. M., Go, Y. M., Samali, A., and Jones, D. P. (2005) Compartmental oxidation of thiol-disulphide redox couples during epidermal growth factor signalling, *Biochem. J. 386*, 215−219.
53. Garcia De La Torre, J., Huertas, M. L., and Carrasco, B. (2000) Calculation of hydrodynamic properties of globular proteins from their atomic-level structure, *Biophys. J. 78*, 719−730.
54. Cantor, C. R., and Schimmel, P. R. (1980) *Biophysical Chemstry*, Part II, W. H. Freeman and Company, San Francisco.
55. Tsodikov, O. V., Record, M. T., Jr., and Sergeev, Y. V. (2002) Novel computer program for fast exact calculation of accessible and molecular surface areas and average surface curvature, *J. Comput. Chem. 23*, 600−609.
56. Lowther, W. T., Weissbach, H., Etienne, F., Brot, N., and Matthews, B. W. (2002) The mirrored methionine sulfoxide reductases of *Neisseria gonorrhoeae* pilB, *Nat. Struct. Biol. 9*, 348−352.
57. Ezraty, B., Bos, J., Barras, F., and Aussel, L. (2005) Methionine Sulfoxide reduction and assimilation in *Escherichia coli*: New role for the biotin sulfoxide reductase BisC, *J. Bacteriol. 187*, 231−237.
58. Kauffmann, B., Aubry, A., and Favier, F. (2005) The three-dimensional structures of peptide methionine sulfoxide reductases: current knowledge and open questions, *Biochim. Biophys. Acta. 1703*, 249−260.
59. Sharov, V. S., and Schoneich, C. (2000) Diastereoselective protein methionine oxidation by reactive oxygen species and diastereoselective repair by methionine sulfoxide reductase, *Free Radic. Biol. Med. 29*, 986−994.
60. Chen, B., Mayer, M. U., and Squier, T. C. (2005) Structural uncoupling between opposing domains of oxidized calmodulin underlies the enhanced binding affinity and inhibition of the plasma membrane Ca-ATPase, *Biochemistry 44*, 4737−4747.
61. Gao, J., Yao, Y., and Squier, T. C. (2001) Oxidatively modified calmodulin binds to the plasma membrane Ca-ATPase in a nonproductive and conformationally disordered complex, *Biophys. J. 80*, 1791−1801.
62. Sacksteder, C. A., Whittier, J. E., Xiong, Y., Li, J., Galeva, N., Jacoby, M. E., Purvine, S., Williams, T. D., Rechsteiner, M. C., Bigelow, D. J., and Squier, T. C. (2006) Tertiary structural rearrangements upon oxidation of Methionine145 in calmodulin promotes targeted proteasomal degradation. *Biophys. J. 91*, 1480−1493.
63. Whittier, J. E., Xiong, Y., Rechsteiner, M. C., and Squier, T. C. (2004) Hsp90 enhances degradation of oxidized calmodulin by the 20 S proteasome. *J. Biol. Chem. 279*, 46135−46142.
64. Petropoulos, I., Mary, J., Perichon, M., and Friguet, B. (2001) Rat peptide methionine sulphoxide reductase: cloning of the cDNA, and down-regulation of gene expression and enzyme activity during aging. *Biochem. J. 355*, 819−825.
65. Toda, T., Morimasa, T., Kobayashi, S., Nomura, K., Hatozaki, T., and Hirota, M. (2003) A proteomic approach to determination of the significance of protein oxidation in the ageing of mouse hippocampus. *Appl. Genomics Proteomics 2*, 43−50.
66. Balog, E. M., Norton, L. E., Bloomquist, R. A., Cornea, R. L., Black, D. J., Louis, C. F., Thomas, D. D., and Fruen, B. R. (2003) Calmodulin oxidation and methionine to glutamine substitutions reveal methionine residues critical for functional interaction with ryanodine receptor-1. *J. Biol. Chem. 278*, 15615−15621.
67. Balog, E. M., Norton, L. E., Thomas, D. D., and Fruen, B. R. (2006) Role of calmodulin methionine residues in mediating productive association with cardiac ryanodine receptors. *Am. J. Physiol. Heart Circ. Physiol. 290*, H794−799.
68. Richardson, J. S., and Richardson, D. C. (1989) *Principles and Patterns of Protein Conformation in Prediction of Protein Structure and the Principles of Protein Conformation*, Plenum Press, New York.
69. Levine, R. L., Mosoni, L., Berlett, B. S., and Stadtman, E. R. (1996) Methionine residues as endogenous antioxidants in proteins. *Proc. Natl. Acad. Sci. U.S.A. 93*, 15036−15040.
70. Chen, B., Mayer, M. U., Markillie, L. M., Stenoien, D. L., and Squier, T. C. (2005) Dynamic motion of helix A in the amino-terminal domain of calmodulin is stabilized upon calcium activation, *Biochemistry 44*, 905−914.
71. Wood, M. J., Helena Prieto, J., and Komives, E. A. (2005) Structural and functional consequences of methionine oxidation in thrombomodulin. *Biochim. Biophys. Acta 1703*, 141−147.
72. Ciorba, M. A., Heinemann, S. H., Weissbach, H., Brot, N., and Hoshi, T. (1999) Regulation of voltage-dependent K+ channels by methionine oxidation: effect of nitric oxide and vitamin C, *FEBS Lett. 442*, 48−52.
73. Santarelli, L. C., Wassef, R., Heinemann, S. H., and Hoshi, T. (2006) Three methionine residues located within the regulator of conductance for K+ (RCK) domains confer oxidative sensitivity to large-conductance Ca2+-activated K+ channels, *J. Physiol. 571*, 329−348.
74. Levine, R. L., Berlett, B. S., Moskovitz, J., Mosoni, L., and Stadtman, E. R. (1999) Methionine residues may protect proteins from critical oxidative damage, *Mech Ageing Dev. 107*, 323−332.
75. Sun, H., Gao, J., Ferrington, D. A., Biesiada, H., Williams, T. D., and Squier, T. C. (1999) Repair of Oxidized Calmodulin by Methionine Sulfoxide Reductase Restores Ability To Activate the Plasma Membrane Ca-ATPase, *Biochemistry 38*, 105−112.
76. Sun, H., Yin, D., Coffeen, L. A., Shea, M. A., and Squier, T. C. (2001) Mutation of Tyr138 disrupts the structural coupling between the opposing domains in vertebrate calmodulin, *Biochemistry 40*, 9605−9617.
77. Yin, D., Kuczera, K., and Squier, T. C. (2000) The sensitivity of carboxyl-terminal methionines in calmodulin isoforms to oxidation

by H(2)O(2) modulates the ability to activate the plasma membrane Ca-ATPase, *Chem. Res. Toxicol. 13*, 103−110.
78. Yin, D., Sun, H., Ferrington, D. A., and Squier, T. C. (2000) Closer proximity between opposing domains of vertebrate calmodulin following deletion of Met(145)-Lys(148), *Biochemistry 39*, 10255−10268.
79. Anbanandam, A., Bieber Urbauer, R. J., Bartlett, R. K., Smallwood, H. S., Squier, T. C., and Urbauer, J. L. (2005) Mediating molecular recognition by methionine oxidation: conformational switching by oxidation of methionine in the carboxyl-terminal domain of calmodulin, *Biochemistry 44*, 9486−9496.
80. Toda, H., Yazawa, M., Sakiyama, F., and Yagi, K. (1985) Amino acid sequence of calmodulin from wheat germ, *J. Biochem. (Tokyo) 98*, 833−842.
81. Chattopadhyaya, R., Meador, W. E., Means, A. R., and Quiocho, F. A. (1992) Calmodulin structure refined at 1.7 Å resolution, *J. Mol. Biol. 228*, 1177−1192.
82. Guex, N., and Peitsch, M. C. (1997) SWISS-MODEL and the Swiss-PdbViewer: an environment for comparative protein modeling, *Electrophoresis 18*, 2714−2723.

BI0612465